UDC 535.372; 535.341.5; 535.016

ACTIVE MEDIUM FOR DYE-LASERS BASED ON A MATRIX OF POROUS Al_2O_3 WITH Ag NANOPARTICLES

Zeinidenov A.K., Ibrayev N.Kh., Aimukhanov A.K.

Institute of Molecular Nanophotonics, Karaganda State University named after E.A. Buketov, Karaganda, Kazakhstan, a_k_aitbek@mail.ru

In this work the luminescent properties of anodized alumina oxide films with high-ordered structure, doped with Rhodamine dyes molecules were investigated. The fluorescence quantum yield in alumina oxide films of Rhodamine 6 G was equal to F_{fl} = 0.78 and Rhodamine B was equal to F_{fl} = 0.54. Stimulated emission of the Rhodamine 6G and Rhodamine B molecules in the film of anodic aluminum oxide is observed. The presence of Ag NPs in porous alumina leads to the decreasing of the dye generation threshold. For Rhodamine B plasmon effect of silver NPs on the stimulated emission is lower than for Rhodamine 6G. This may be due to the smaller overlap of absorption and fluorescence spectra of the dye and Ag NPs in the matrix of the alumina.

Keywords: Ag nanoparticulars, anodized alumina oxide films, dyes molecules, stimulated emission, plasmon effect.

Introduction

Researches related to the excitation of localized plasmon resonance of metal nanoparticles have most interest in recent times [1,2]. Surface-enhanced Raman scattering is the most famous among the optical manifestations of localized plasmon resonance [3]. Molecules of luminophores placed near the surface of metal nanostructure also undergo the action of the local electro-magnetic fields. Thus, depending on the distance between the nanoparticles and molecule fluorescence of the past could be enhanced or quenched [4,5]. Emission could be quenched at close distances and direct contact of nanoparticles with fluorophores. Practically, interest in the plasmonic effect is linked to the possibility of the creation of highly sensitive sensors [6], optoelectronic devices [7], lasers [8], photovoltaic cells [9]. The addition of metal nanoparticles in the active medium of dye lasers leads to the lowering in the generation threshold [10,11,12]. The results of studying the stimulated emission in a thin film of nanoporous aluminum oxide doped with Rhodamine 6 G dye and Ag nanoparticles we are presented. The choice of porous alumina is due to the fact that the alumina oxide has many advantages: chemical, thermal stability, transparency in the visible region of the spectrum, and excellent adsorptive properties due to a large volume of pores having a branched surface [13,14]. Fluorescent properties of dyes embedded in the pores of alumina oxide were studied in [15,16]. In the [17], a porous alumina matrix was used for formation of active laser nanofibers of poly(9-vinylcarbazole) doped with TiO_2 particles and Rhodamine 6 G. OLEDs based on anodic porous alumina were obtained in [18]. In [19], a nanoporous alumina matrix with Ag nanoparticles was proposed for use as Raman scattering active mediums. It has been shown [20] that the anodic alumina membranes are promising material for high-tech devices that operate at high temperatures. The porous anodic aluminum oxide structure undergoes no substantial change and remains stable over a wide temperature range up to 1000°C. The heat conductivity factor of aluminum oxide films is equal to 1.6 Wm^{-1} K^{-1} which is significantly higher than the thermal conductivity of polymeric materials and glass used as solid-state active elements in tunable dye lasers [21]. Using the matrix of the porous alumina will contribute to the rapid dissipation of heat, which occurs upon absorption of light by the process of internal conversion in the dye molecules.

1. Experimental part

Synthesis of alumina was carried out on 'mild' anodizing conditions including two-stage synthesis at low values of the voltage (U = 40 V) in a solution of 0.3 M oxalic acid [22]. For electrochemical synthesis of nanoporous alumina as a starting material the aluminium plates (purity is 99.99 %) with a thickness of 0.5 mm and dimensions of 3.5 × 3.5 cm have been used.

To increase the size of crystallites of aluminum and removal of microstrains in the sample and the subsequent order best distribution received pore alumina substrate was annealed in a muffle furnace in air for 10 hours at T = 500 ° C. To remove surface defects of aluminum the sample was prone to electrochemical polishing in a pulsed mode in a solution of CrO_3 and H_3PO_4. Thereafter, the samples were washed in distilled water and air dried. Silver NP were obtained by reduction $AgNO_3$ in porous alumina [19]. The sorption of the dyes Rhodamine 6 G and Rhodamine B molecules in the pores was carried out by exposing the alumina films in aqueous solution.

Spectral characteristics of stimulated emission were studied upon second harmonic excitation of samples by Nd: YAG laser (SOLAR LQ 215, λ_{gen} = 532 nm, E_{imp} = 90 mJ, τ = 10 ns) in the longitudinal version. A resonator was formed with two glass plates where the film was placed. The pumping radiation passing a diaphragm by means of lenses is focused on the surface of the film in the dots with the area of 0.13 cm^2. Pump power density was varied with the help of a neutral density filter and was equal to 0.01^{-1} MW cm^{-2}. The stimulated emission of a film by means of a collecting lens was focused on an entrance of an optical fibre of a spectrometer of AvaSpec-2048 (fig. 1).

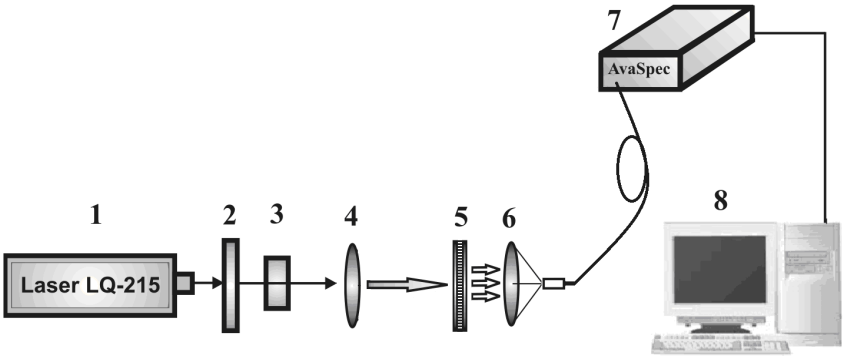

Fig. 1. Installation for investigating the characteristics of stimulated emission of thin films:.
1 – LQ 215; 2 – neutral density filters; 3 – diaphragm; 4.6 – lens; 5 – sample; 7 – AvaSpec-2048;
8 – computer

2. Results and its discussing

The surface morphology and cross-cleaved samples obtained in a scanning electron microscope MIRA 3LMU are shown in figure 2. The measurements was carried out at accelerate voltage of 7 kV and working distance of 7 mm in high vacuum. One can see on the film surface uniform pores of diameter ~ 80 nm and the distance between the pores of approximately 105 nm (figure 2(a)) are observed. On the cross-cleaved sample (figure 2(b)) the parallel straight channels arranged perpendicularly to the surface are visible. It is could be well defined that as the result of the synthesis silver nanoparticles formed on the surface and pore walls.

The absorption and fluorescence spectra of Rhodamine 6 G embedded in the channels of porous matrix exhibits the maximum at 524 nm (figure 3 curve 2). The main maximum of the fluorescence spectrum is observed at 566 nm (figure 3 curve 3). The absorption and fluorescence spectra of Rhodamine B embedded in the porous matrix exhibits the maximum at 556 nm and 596 nm correspondingly.

.

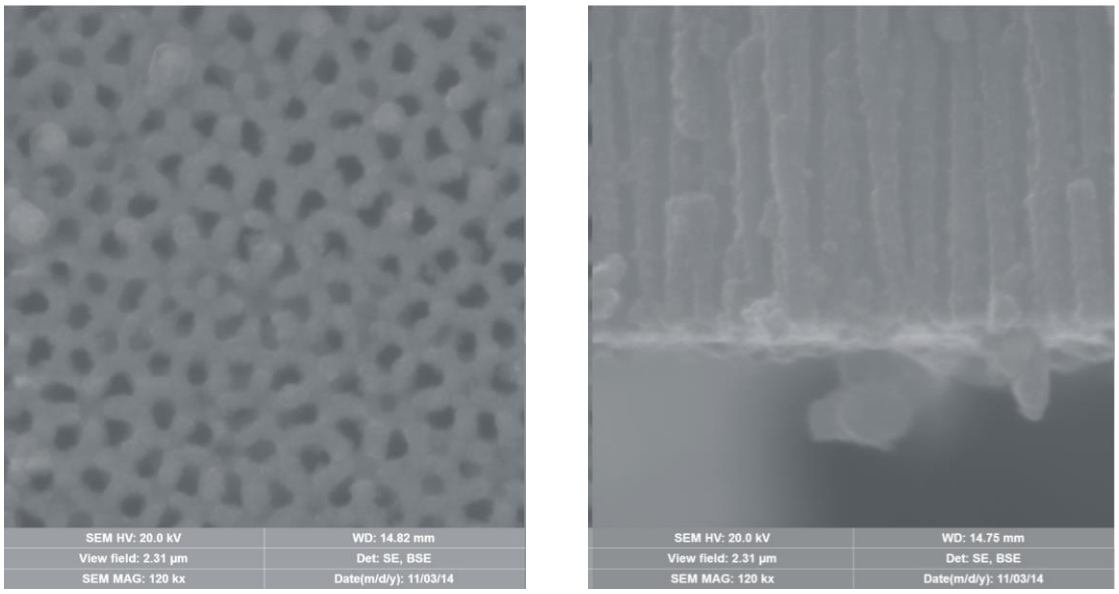

a) b)

Fig. 2. The SEM images of the porous alumina film (a) and bottom side of the oxide film after chemical reduction of the Ag NPs.

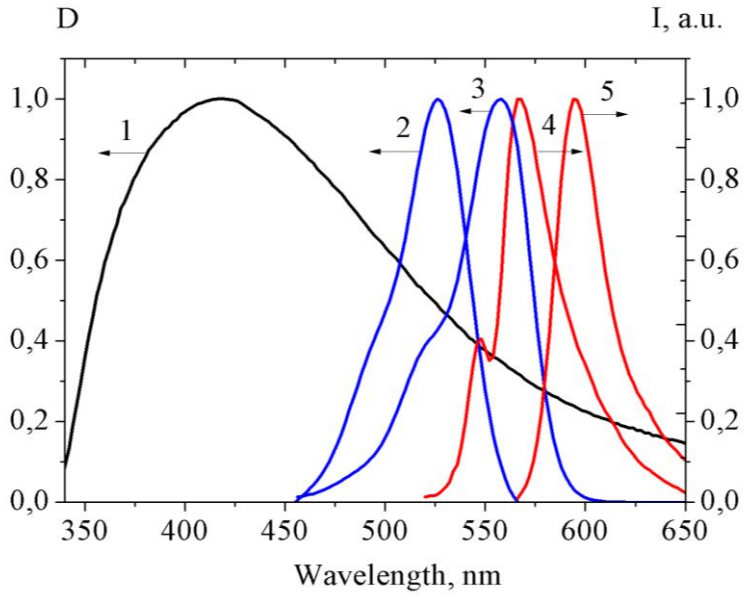

Fig.3. Absorption and fluorescence spectra of dye molecules and Ag NPs embedded in the pores of alumina

The absorption spectra of Ag nanoparticulars embedded in the porous matrix exhibits the maximum at 412 nm (figure 3 curve 1) and overlaps with the absorption and fluorescence spectra of dyes. It is evidence of the conditions of plasmon resonance. It should be noted that the overlap spectra of Rhodamine B with Ag NPs is smaller than for the Rhodamine 6G. The quantum yield of fluorescence (F_{fl}) of Rhodamine 6G and Rhodamine B molecules in the pores of alumina was determined by de Mello absolute method for hybrid systems. The fluorescence quantum yield of Rhodamine 6 G was equal to $F_{fl} = 0.78$ and Rhodamine B was equal to $F_{fl} = 0.54$.

Stimulated emission of the Rhodamine 6G and Rhodamine B molecules in the film of anodic aluminum oxide is shown in figure 4. When the power density of the pump source is equal to P = 0.2 MW cm^{-2} only the spectrum of the spontaneous fluorescence with maximum at 566 nm Rhodamine 6G (figure 4 curves 1) was observed. Increasing the power of the pump source up to

0.38 MW cm^{-2} leads to the appearance of a narrow band with a maximum 566 nm wavelength on the background of the laser-induced fluorescence spectrum, which refers to the band of the stimulated emission [23]. The narrowing of the emission band with increasing of excitation intensity indicates the predominance of stimulated emission over spontaneous emission. The system switch over to generation mode.

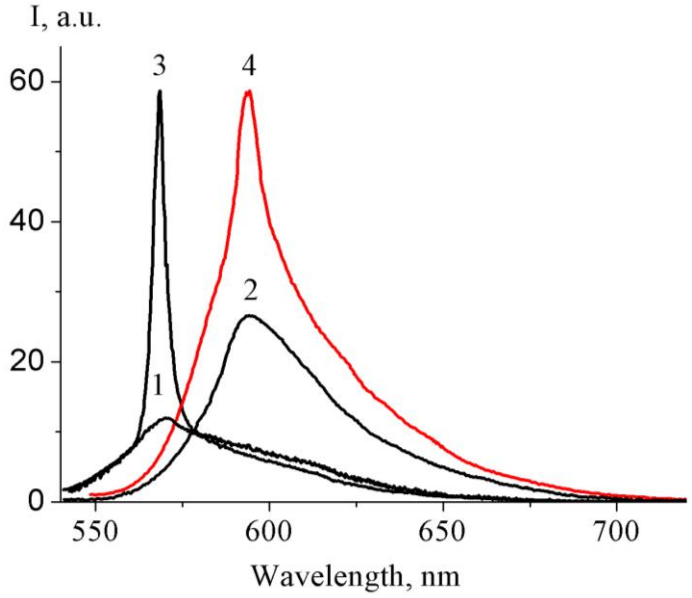

Fig. 4. Influence Ag nanoparticles on the spectra of stimulated emission of Rhodamine 6G (1.3) (P <0.38 MW / cm^2) and Rhodamine B (2.4) (P <0.44 MW / cm^2) in the anodic alumina.

For the Rhodamine B when the power density of the pump source is equal to P = 0.3 MW cm^{-2} only the spectrum of the spontaneous fluorescence with maximum at (figure 4 curves 2) was observed. Increasing the power of the pump source up to 0.44 MW cm^{-2} leads to the appearance of a narrow band with a maximum 596 nm wavelength of the stimulated emission. Further increasing of pump density power lead to growth of intensity and narrowing of the band of stimulated emission of dyes.

The appearance of stimulated emission in the case of using resonator with low quality factor due to the fact that to the Fresnel reflection from two glass plates the cylindrical microcavities of the matrix serves as microresonators. Due to the effect of total internal reflection of electromagnetic waves from the walls of the pores in the microcavity concentrated high energy density of the electromagnetic field, which greatly strengthens the emission intensity of the dye molecules in the pores.

If the value of the power density of the pump source below the threshold in the samples with silver NPs stimulated emission spectrum of the dyes in the anodic aluminum oxide (figure 4 curves 3 and 4) is observed. Influence of the power density of the pump source on the intensity and half-width of the spectrum of stimulated emission of Rhodamine 6G in the anodic alumina with Ag NPs shown in figure 5a.

The intensity in the maximum spectra upon changing of the power density of the pump source from 0.1 to 0.8 MW / cm^2 increased by 3.4 times and the half-width in the emission spectrum is narrowed by 3 times for the sample with the Ag NPs. Comparison of experimental data for samples with Ag NPs and without them shows the correlation between changes in the intensity and half-width of the emission spectrum. From the data shown in the figure 5 it is evidence a decrease in the lasing threshold in the presence of pores in the alumina Ag NPs. For a film with Ag NPs lasing threshold is reduced by 2.2 times.

.

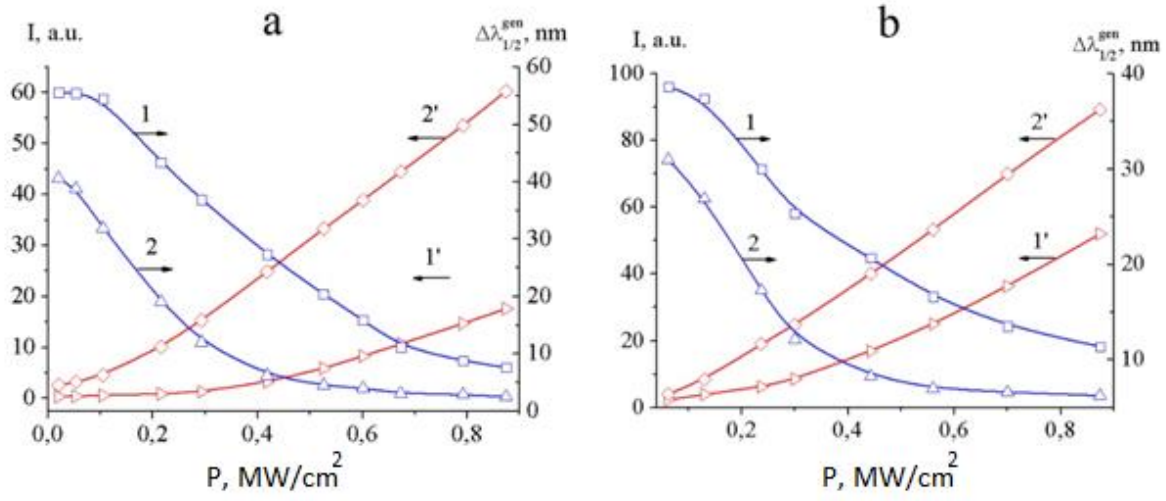

1, 1' - without Ag NPs, 2, 2' - with Ag NPs

Fig. 5. Depending on the intensity and half-width of the emission spectrum of Rhodamine 6G (a) and Rhodamine B (b) in the porous anodic alumina of the pump power density.

In the case of Rhodamine B intensity of emission increases by 1.7 times and the half-width of the spectra is narrowed by 1.7 times. Lasing threshold of stimulated emission is reduced by 1.4 times. The parameters of stimulated emission of Rhodamine 6G and Rhodamine B in the pores of alumina are shown in Table 1.

Table 1. Influence of Ag nanoparticles in the pores of anodized aluminum on the parameters of stimulated emission spectra of Rhodamine 6G and Rhodamine B.

Dye	λ_{max}^{abs}, nm	$\Delta\lambda_{1/2}^{abs}$, nm	λ_{max}^{fl}, nm	$\Delta\lambda_{1/2}^{fl}$, nm	F_f	λ_{max}^{gen}, nm	$\Delta\lambda_{1/2}^{gen}$, nm	Threshold of generation, MW/cm^2
Rhodamine 6G without Ag NPs	524	42	566	58	0.78	566	23	0.38
Rhodamine 6G with Ag NPs	524	42	566	43	-	566	3.5	0.17
Rhodamine B without Ag NPs	556	46	596	38	0.54	594	20	0.44
Rhodamine B with Ag NPs	556	46	596	31	-	594	12	0.3

Conclusion

Thus, in this work the luminescent properties of anodized alumina oxide films with high-ordered structure, doped with Rhodamine dyes molecules were investigated. The fluorescence quantum yield of the Rhodamine 6G and Rhodamine B in the matrix of the alumina is equal to 0.78 and 0.54 correspondingly. Generation of stimulated emission of dye molecules in the film of anodized aluminum oxide was obtained. For Rhodamine 6G it is determined that under excitation of the samples with the pump source power density of 0.1 MW cm^{-2} the spectrum of the laser-induced fluorescence of the dye is only observed. When the power of the pump source reaches 0.38 MW cm^{-2} on the background of laser-induced fluorescence spectrum the narrow band of stimulated

emission with a peak wavelength of 566 nm appears. The presence of Ag NPs in porous alumina leads to the decreasing of the dye generation threshold. For Rhodamine B plasmon effect of silver NP on the stimulated emission is lower than for Rhodamine 6G. This may be due to the smaller overlap of absorption and fluorescence spectra of the dye and Ag NPs in the matrix of the alumina.

ACKNOWLEDGEMENTS

The research was supported by State Research Program "New optically active media based on laser dyes and metallic nanostructures", grant No. 1124/GF4.

REFERENCES

1 Klimov V.V. *Nanoplasmonics.* Fizmatlit, Moscow, 2009, 480 p. [in Russian]

2 Maier S.A. *Plasmonics: Fundamentals and Applications*. Springer, Berlin, 2007, 248 p.

3 Tian Z.Q. Surface–enhanced raman spectroscopy: advancements and applications. *J. Ram. Spect.*, 2005, Vol. 36, pp. 466 – 470.

4 Lakowicz J.R. Release of the self–quenching of fluorescence near silver metallic surfaces. *Analytical Biochemistry*. 2003, Vol. 320, pp. 13-20.

5 German A.E., Gachko G.A. Dependence of the amplification of giant Raman scattering and fluorescence on the distance between an adsorbed molecule and a metal surface. *J Appl Spectrosc.* 2001, Vol. 68, pp.987-990.

6 Homola J., Yee S.S., Gauglitz G. Surface plasmon resonance sensors: review. *Sens Actuators B Chem.* 1999, Vol. 54, pp.3-15.

7 Novotny L. *Principles of Nano-Optics*. Cambridge University Press, Cambridge. 2006, 481p.

8 Oulton R.F. Plasmon lasers at deep subwavelength scale. *Nature*. 2009, Vol. 461, pp. 629 -632.

9 Vedraine S., Gernigon V., Torchio Ph., Flory F., Heiser T., Leveque P., Escoubas L. Surface Plasmon Effect on Metallic Nanoparticles Integrated in Organic Solar Cells. *Proc. of the conf. SPIE*, 2011, Vol. 172, pp. 1-7.

10 Vasa P., Pomraenke R., Schwieger S., Mazur Y.I., Kunets V., Srinivasan P., Johnson E., Kihm J., Kim D., Runge E. Coherent exciton–surface–plasmonpolariton interaction in hybrid metal–semiconductor nanostructures. *Phys. Rev. Lett.* 2008, Vol. 101, 116801.

11 Kim J.W., Lee J.E., Kim S.J., Lee J.S., Ryu J.H., Kim J., Han S.H., Chang I.S., Suh K.D. Synthesis of silver/polymer colloidal composites from surface–functional porous polymer microspheres. *Polymer*. 2004, Vol. 45, pp. 4741.

12 Noginov M.A., Zhu G. The effect of gain and absorption on plasmons in metal nanoparticles surface. *Appl. Phys. B.* 2007, Vol. 86, pp. 455.

13 Golovan L.A., Timoshenko V.Yu., Kashkarov P.K. Optical properties of porous-system-based nanocomposites. *Prog. Phys. Sci.* Papers 2007, Vol. 6, pp. 619.

14 Thompson G.E., Xu Y., Skeldon P., Shimizu K., Han S.H., Wood G.C. Optical and structural characterization of erbium–doped TiO2 xerogel films processe on porous anodic alumina. *Philos. Mag. B.* 1987, Vol. 55, pp. 651.

15 Zhang Z.L., Zheng H.R., Dong J., Yan X.Q., Sun Y., Xu H.X. Surface enhanced fluorescence by porous alumina with nanohole arrays. *Science China physics, mechanics and astronomy*. 2012, Vol. 55, pp. 767.

16 Moadhena A., Elhouicheta H., Nosovab L., Oueslatia M. Rhodamine B absorbed by anodic porous alumina: Stokes and anti–Stokes luminescence study. *Journal of luminescence*. 2007, Vol. 126, pp. 789.

17 Shin H.W., Cho S.Y., Choi K.H., Oh S.L., Kim Y.R. Directional random lasing in dye–TiO2 doped polymer nanowire array embedded in porous alumina membrane. *Applied Physics Letters*. 2006, Vol. 88, pp. 1-3.

18 Kukhta A.V., Gorokh G.G., Kolesnik E.E., Mitkovets A.I., Taoubi M.I., Koshin Yu.A., Mozalev A.M. Nanostructured alumina as a cathode of organic light–emitting devices. *Surface Science*. 2002, Vol. 507, pp. 593.

.

19 Mondal B., Saha S.K. Fabrication of SERS substrate using nanoporous anodic alumina template decorated by silver nanoparticles. *Chemical Physics Letters*. 2010, Vol. 497, pp. 89.

20 Lee J., Kim Y., Jung U., Chung W. Synthesis of silver/polymer colloidal composites from surface–functional porous polymer microspheres. *Mater. Chem. Phys.* 2013, Vol. 141, pp. 680

21 Assael M.J., Botsion S., Gialou K., Netaxa I.N. Thermal conductivity of polymethyl methacrylate (PMMA) and borosilicate crown glass BK7. *Int. J. Thermophys.* 2005, Vol. 26, pp. 1595.

22 Nielsch K., Choi J., Schwirn K. *Self–ordering regimes of porous alumina: The 10% porosity rule. Nano Letters*. 2002, Vol. 2, pp. 677.

23 Ibrayev N.Kh., Zeinidenov A.K. Plasmon–enhanced stimulated emission of Rhodamine 6G in nanoporous alumina. *Laser Physics Letters*. 2014, Vol. 11, pp. 115805.

Article accepted for publication 28.03.2017